Coverage Optimization with Non-Actuated, Floating Mobile Sensors using Iterative Trajectory Planning in Marine Flow Fields

Johanna Hansen[1] and Gregory Dudek[1]

***Abstract*— This paper considers a spatial coverage problem in which a network of passive floating sensors is used to collect samples in a body of water. We employ an iterative measurement and modeling scheme to incrementally deploy sensors so as to achieve spatial coverage, despite only controlling the initial sample point. Once deployed, sensors are moved about a survey area by ambient surface currents. We demonstrate our results in simulation on 40 different ocean flow fields and compare against several baselines. This work provides a computational tool for scientists seeking a low-cost, autonomous marine surveying system. Although in this paper, we concentrate on ocean drifters, our approach can be extended to other domains where a spatial distribution of passive nodes in a flow field can be modeled.**

I. Introduction

Scientific understanding of spatiotemporal phenomena in bodies of water is key to preserving the health of marine ecosystems, but the nature of these systems make them expensive to sample at a high resolution. In this paper we describe our approach for serially deploying inexpensive, non-actuated sensors to maximize spatial coverage with minimal investment in infrastructure. Our floating sensors, called *drifters*, are propelled only by the ambient surface currents in the water upon deployment (illustrated in Figure 2). These devices, equipped with any number of sensors (such as temperature, pH, or cameras), sample the local environment and wirelessly report geotagged data back to a central server. The approach discussed in this paper is to collect measurements in as many cell of an evenly gridded measurement area as possible in a limited amount of time, not necessarily to gather high-entropy samples.

In typical self-propelled robotic systems, exogenous (external) forces are usually thought of as an antagonistic influence to be counteracted and overcome. In deployed drifter systems, however, external forces are the propulsive mechanism that we exploit to achieve our objectives. This paper discusses and provides a solution for incrementally estimating these flow fields in real time from limited local observations and then harnesses those estimates to effectively cover a sample space by selecting valuable deployment locations.

*We would like to thank the the Natural Sciences and Engineering Research Council (NSERC) for their support through the Canadian Field Robotics Network (NCFRN).

[1]Mobile Robotics Lab at the Centre for Intelligent Machines at McGill University, Montreal, QC, Canada jhansen,dudek@cim.mcgill.ca

Submitted to the 2018 IEEE/RSJ International Conference on Intelligent Robots and Systems.

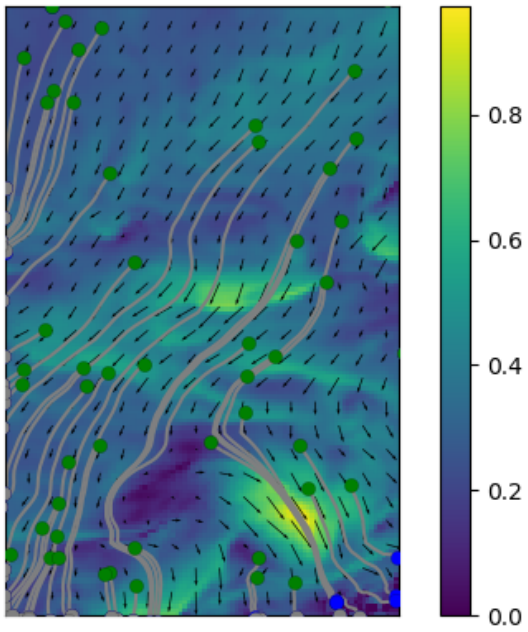

Fig. 1: These drifters were deployed randomly over a flow field to illustrate sample trajectories. Simulated trajectories, like the ones depicted here, will be drawn throughout the paper as gray points with the trajectory start denoted by a green marker and the trajectory termination denoted by a blue marker (not always seen). The flow field direction is described in each grid cell by an arrow. Speed is represented by the colormap in m/s according to the attached colorbar. This particular flow field is one of 40 used for evaluation and serves as the ground truth flow field, $\vec{V}$, for Figures 2 and 4.

The concept of the drifting data collector, perhaps beginning with the message in a bottle [1], has long been employed to gather information about bodies of water. Modern drifters are widely used in oceanographic studies because of their low cost and suitability for long-term sampling missions [2]. The largest network of drifters, The Global Drifter Program, has been conducting global-scale data collection in the world's oceans for nearly 30 years [3]. This program's 1200 operational drifters report a plethora of scientific readings that have been integral in building and validating ocean models [4] and informing transport calculations of other passive particles such as marine debris [5] and radioactive contaminants [6].

II. Problem Statement

Traditional marine surveying schemes typically lack spatial or temporal resolution (and sometimes both) because

of the expense associated with continuously sampling harsh marine environments. Most surveying systems involve a tradeoff between cost, mobility, and resolution in time and space. One traditional approach to marine sensing consists of deploying an array of static sensors throughout a survey space such as in [7]. This deployment method can take measurements often (depending on power constraints), but is usually too costly to deploy at a high spatial resolution and can be difficult to move to new locations. Other techniques employ sophisticated robots, such as autonomous surface vehicles (ASVs) or autonomous underwater vehicles (AUVs). These robots can collect data at high-spatial resolutions in an exhaustive [8], [9] or selective [10] manner. Although potentially effective, approaches based on using sophisticated mobile vehicles tend to be too expensive for most routine applications and environments.

The surveying approach presented in this paper seeks to offer a hybrid alternative to the previously mentioned methods by providing a moderate resolution sampling method with low overhead. Though a drifter network's low cost is what makes it an attractive approach for marine sampling, its simplicity also makes it a difficult platform from which to sample efficiently. A traditional drifter's initial deployment point is the only controlled movement. The remaining sample trajectory, and thus the amount of the survey area covered by the sensor, is dictated by the ambient flow field. When a drifter in a drifter network is poorly deployed or confronted with unstable currents, it can become trapped in an eddy or quickly rushed out of a survey area, collecting redundant or few samples for the survey. Thus, the need for a strategic deployment is necessary to achieve any form of efficient coverage with drifters. This was clear in our earlier work, [11], in which we introduced an adaptive sampling technique that relied on deployed drifters for scouting for an ASV. In these experiments, the drifters tended to clump together or rapidly exit the survey area, reducing their utility.

Previous work [12] has shown that drifter trajectories can be modeled effectively with an accurate flow field representation. However, at the scale we are working ($< 5km^2$ survey region with sample resolution of $< 20m$), the flow field for most bodies of water is largely unknown before the survey begins and is only observable in-situ. Even if a full dynamic model of the flow field is known, the question of optimal drifter placement remains. An exhaustive placement search could be performed through the known flow field with a particle trajectory simulator, however, this search is generally too costly to perform in real-time deployments. In the sections that follow, we describe our approach to overcoming these two limitations and present a method for non-actuated sensor coverage optimization in partially observed flow fields which is able to run in a real time system.

III. Related Work

Much of the previous work on coverage and deployment of sensor systems assumes either an environment where agents are able to move deliberately [13] or systems in which only initial placement in a static environment is considered [14] [15]. We herewith discuss related work in trajectory planning in marine flow fields, ordered from full-actuation to passive systems. In [16], [17], the authors present methods for tracking features of interest by utilizing the output of predictive ocean models. Kulartne et al. [18] find energy efficient motion plans in flow fields for fully-actuated vehicles using graph search methods. Several authors have also considered the use, search, and interception of drifting sensor devices [19], [11], [20], [21].

Perhaps more relevant to our work are systems which enable underactuated vehicles to strategically move through flow fields. These situations impose limitations on planning which make initial deployment points important. In [22], Pereira et al. present techniques for risk-aware path planning techniques with AUVs navigating in strong currents, utilizing regional ocean models to avoid trajectories where collision is more likely. In [23], the authors describe a performance metric for determining optimal paths with self-directed underwater gliders, which minimizes the error in the model estimate of the sampled field. In [24], Innac et al. demonstrate an approach to optimal trajectory planning for an underwater glider using Lagrangian Coherent Structures with global flow geometry based on approximate ocean current models.

Active drifters, which have some limited ability to influence their trajectory, have become more prominent in recent years and are an interesting tool for strategic sampling. In [25] active underwater drifters alter their depth to use ocean flow fields that are carefully modeling in advance for coordinated rendezvous to enable efficient recovery. The active drifters system proposed in [26] by Molchanov et al. performs spreading and aggregation in an ocean simulation model by lowering or raising individual drifter drogues to take advantage of ocean currents measured in-situ by individual drifters. These systems are capable of performing the task of planning their trajectory to reach a goal point.

Others within the oceanographic community have looked at the effect a deployment location has on a drifter's trajectories for long-term ocean deployments. The following studies informed our approach for our medium-scale autonomous system. In [27], Molcard et al. showed that directing the initial drifter positions along the out-flowing branch of Lagrangian boundaries optimized relative dispersion of drifters. This work also demonstrated that the performance of drifter data assimilation into ocean models strongly depends on the independence of the observed drifter trajectories. In [12], the authors compare long-term multi-drifter deployment strategies and show how different release formations effect data assimilation performance. They demonstrate global error reduction which requires dispersion of drifters, but local errors are reduced by targeting specific flow features. Our deployment proposal process, described in Section IV-C, prefers points which have poorly modeled, thus often selects deployment points described as favorable in [27] and [12].

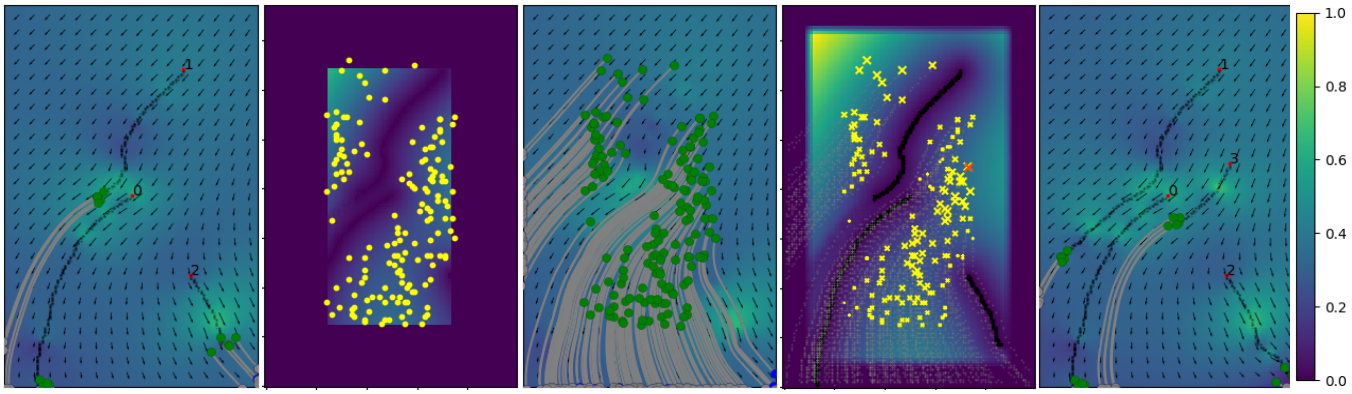

(a) Estimate flow field (b) Generate points (c) Find trajectories (d) Evaluate points (e) Deploy next drifter (f)

Fig. 2: This sequence of figures details the steps performed to determine a deployment point for a fourth drifter into a partially observed flow field. The true flow field is shown in Figure 1, however at the decision point depicted in Figure 2a, we have only observed a small portion of the survey area. These flow field observations, $\bar{O}$, are shown with black dots. Initial deployment points are shown by numbered red dots. These current observations were assimilated into an estimate of the flow field, $\hat{V}$, which is shown in the background of Figure 2a. We use $\hat{V}$ to estimate possible future trajectories (shown in grey points in Figure 2a) from the last observed position for each deployed drifter (green dots). These future trajectories, $\hat{D}$, are combined with previously observed points, $\bar{D}$, uncertainty, U, and an edge mask to build a heuristic field over R that describes a preference for deployment points. From this *preference field*, Φ, (seen in the colormap of Figure 2b), we sample n_p proposal points, p, (yellow points) for evaluation. Next, we estimate possible trajectories for these points with $\hat{V}$ as shown in Figure 2c. In Figure 2d, we evaluate the trajectories (light grey) of p against the *value field*, Γ, which is depicted in the colormap. Γ is constructed from a combination of U, $\bar{D}$, $\hat{D}$, and a safety buffer, rewarding long trajectories which traverse unseen points. Also in Figure 2d, we show the relative score of the proposal points by the size of their yellow markers. The highest scoring point is marked in red and becomes the deployment point. In the final map in this panel, we show the new $\hat{V}$ after deploying the fourth drifter. The colormaps in Figures 2a, 2c, and 2e colormaps refer to Figure 1's colorbar for flow speed in m/s. The colormaps for Figures 2b and 2d refer to the colorbar in Figure 2f.

IV. Method

In this paper, we consider the problem of finding optimal deployment points for a prescribed number of surface drifters over a flow field such that the number of unique sample locations in a region R is maximized. A flow field is a distribution of velocity over a given region. It is denoted in Euclidean space as $\vec{V} = \vec{V}(x, y, z, t)$, which is a function of coordinates in space (x,y,z) and time (t). Velocity at every point in $\vec{V}$ is defined by components in each coordinate direction as described by $\vec{V} = u\vec{i} + v\vec{j} + w\vec{k}$. Each velocity component (u,v,w) is a function of (x,y,z,t) as defined in Equation 1. For the purposes of this paper, we assume that z is a constant (at the water's surface) and that the vertical current is negligible (when the drifters have substantial positive buoyancy). In addition, we assume that the flow field is a steady flow in that it does not change over our observation window, leaving $\vec{V} = \vec{V}(x, y)$ and $\vec{V} = u\vec{i} + v\vec{j}$.

Before discussing our approach to finding deployment points in a flow field, it is necessary to define terms that will be used throughout the paper. In our system, each deployed drifter is denoted by the time-independent point, d_n, which also describes the drifters initial deployment point in $d_n = (\bar{x}_{init}, \bar{y}_{init})$. A deployed drifter has a trajectory $\bar{D}_n$, which is the collection of the points it has visited in R. The collection of observed samples along $\bar{D}_n$, $(\bar{x}, \bar{y}, \bar{u}, \bar{v})$ is denoted by $\bar{O}_n$. We refer to the collection of trajectories from all deployed drifters as $\bar{D}$ and the collection of observed samples from all deployed drifters as $\bar{O}$. The total number of drifters for a survey is denoted by n_d.

$$\vec{V} = u(x, y, z, t)\vec{i} + v(x, y, z, t)\vec{j} + w(x, y, z, t)\vec{k} \quad (1)$$

Given a perfectly known flow field, $\vec{V}$, and an initial location of point particle, a trajectory of the particle through $\vec{V}$ can be calculated by integrating using the advection equation as a function of time. Given unlimited computation time, we could use the perfect flow field model to estimate future trajectories of drifters which have been deployed throughout R and choose the most appealing point for deployment of the real sensor. This simple approach to drifter deployment is, unfortunately, intractable in real systems due to both the vast number of possible deployment points and the high computational cost of solving for each possible trajectory. Moreover, we lack a perfect model of the flow field model, since we only have isolated measurements at $\bar{O}$. In addition, since our drifters are not point particles, but floating sensors, we realize that we will only imperfectly estimate advection with the help of physical parameter describing drifter shape. These factors make the evaluation of potential deployment points difficult, but the approach we present in the following sections seeks to make the problem tractable. First, we discretize the survey space, R, into $m \times n$ square cells of size r, where r is related to the sample validity of the sensors

used in the drifters.

Our iterative trajectory planning approach picks new deployment points based on estimated futures developed from observations made by deployed drifters. These observations allow us to update our estimate of the flow field, $\hat{V}$ through data assimilation as described in Section IV-A. Instead of calculating trajectories for all points in the flow field, we have developed a process of point proposals (Section IV-C) to reduce the number of trajectories that need to be calculated. We assess the trajectories from proposed points using a scoring mechanism that combines expected improvement of $\hat{V}$ with a parameter that encourages drifter trajectories which observe new points in R. Because we initially have no knowledge of the flow field, we always choose the very center of the survey area as the deployment point for the first drifter.

A. Modeling Flow Fields

Developing a model, $\hat{V}$, of the true flow field, $\vec{V}$, from all observed flow field measurements, $\bar{O}$, is the first step in our pipeline when searching for a new deployment point. The assimilation of drifter velocity measurements into a current model has been widely studied in the oceanography community [28], [29], [30], [31], [32], with most practitioners employing a Bayesian filtering approach to integrating data. We will also take a Bayesian approach, formulating the estimation of unobserved points as a regression problem and utilizing a Gaussian process (GP) to approximate the flow field for the entire survey area. Gaussian processes offer nice properties which make them a common tool for modeling spatiotemporal processes as seen in [33], [34], [35], [36]. In this paper, we utilize an exponential kernel $K(a, a') = \sigma^2 \exp(\frac{(a-a')^2}{2l^2})$, with $\sigma = 1$, $l = .2$. In this notation, l is the *length* parameter which regulates how far the GP will extrapolate from an observed data point. The σ parameter is a scaling factor that determines the average distance the function will be from the mean. The covariance matrix of the GP provides us with a measure of uncertainty, U, of the flow field estimate that describes the similarity between every pair of input points $K(a, a')$. In Sections IV-C and IV-D we will discuss how U is used to encourage exploration into points in R which are not well modeled by $\hat{V}$.

B. Trajectory Predictions

Our deployment scheme seeks to place drifters into an initial position in the flow field which will cause them to cover as many new points in R as possible. We accomplish this by building a model of the flow field as described in the previous section, and then using that model to evaluate potential deployment points. For the advection calculations of drifters in this paper, we use a particle trajectory modeling framework, OpenDrift [37], to estimate likely paths of drifters with given starting points under $\hat{V}$.

Trajectory estimates are computed twice each time we search for a new deployment point. The first estimation is performed to find n_f potential future trajectories from the last known point of each deployed drifter. These future path estimates of the deployed drifters are collectively referred to as $\hat{D}$ and will be used to evaluate proposed deployment point's paths against the futures of drifters which are already deployed. In our experiments, we set $n_f = 4$ and randomly seed a 2 meter location around the last known location of each deployed drifter. The second trajectory estimate is computed over all of the proposed deployment points. These proposal point trajectories, $\hat{P}$ will be scored and ranked as described in Section IV-D to choose the optimal deployment point.

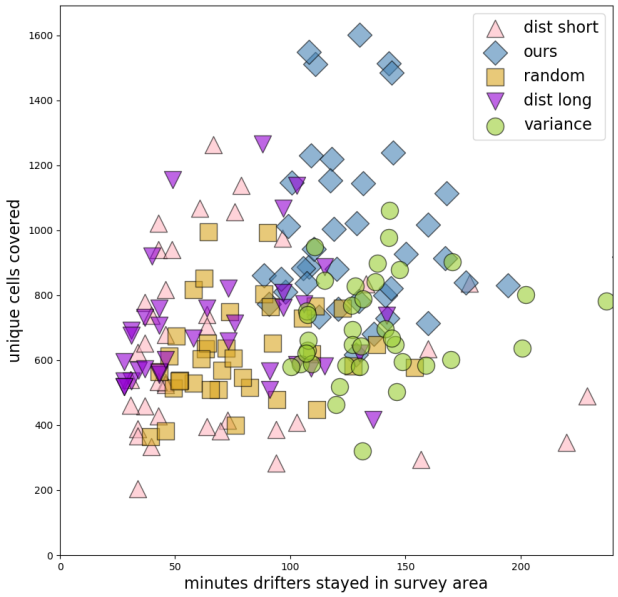

Fig. 3: Performance comparison over 40 flow field maps as described in Section V. Good surveys contain a large number of unique points and have drifters which stay in R for as long as possible (i.e. the top right corner is best). Our deployment scheme performed best in 37 of the 40 schemes we examined.

C. Deployment Point Proposals

We expect flow field estimates of $\hat{V}$ which are near $\vec{V}$ to enable us to more accurately model trajectories. When searching a new deployment point, we must balance the desire to gain new observations which improve our estimate of $\vec{V}$ while still exploiting what we already know about the flow field to achieve long trajectories which cover as many new points of R as possible. However, estimated trajectories which pass through areas where $\hat{V}$ has low confidence (U is high) may be inaccurate, resulting in unpredicted paths which perform poorly. In the following sections, we discuss how we choose d_n to balance our desire to better model $\vec{V}$ with our quest to cover R.

These incentives are realized in a 2D matrix dubbed the *preference field* of size $m \times n$. The preference field, Φ, is initialized to be equal to a normalized U. A receding safety buffer sets points along the edge of R to zero. This receding safety buffer prevents proposals along the edges of R which may be appealing to our sampler because of high values in

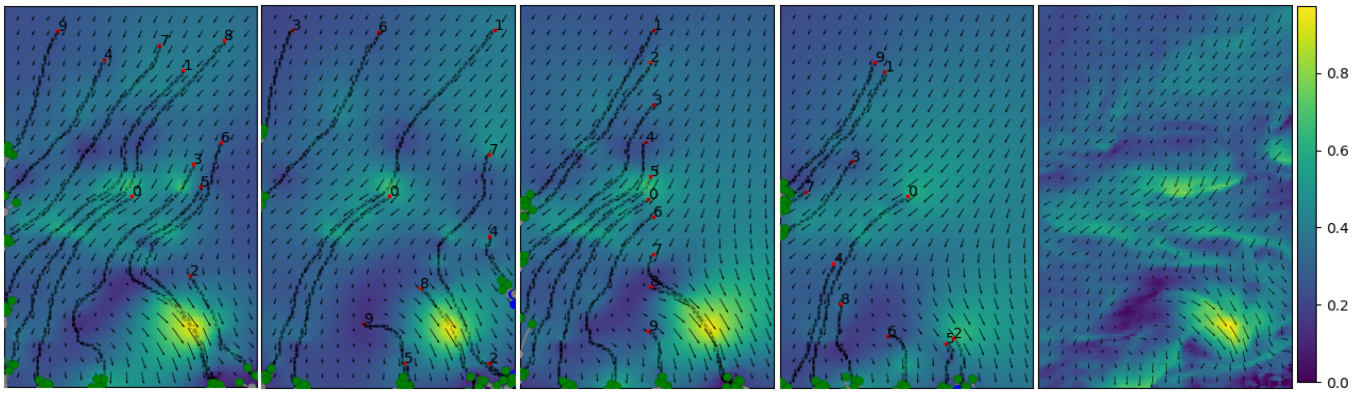

(a) ours (b) variance (c) distributed long (d) random (e) ground truth (f)

Fig. 4: This panel shows the deployments (numbered red points) chosen for 10 drifters under 4 different deployment schemes as discussed in Section V. The true flow field for these experiments is depicted in Figure 1 and also shown in Figure 4e. The background and arrows in the experimental figures depict each deployment scheme's estimate of $\vec{V}$ at the terminal state of the survey. The comparative performance of these strategies in this flow field is shown in Figure 5.

U, but could result in short trajectories when the drifter is actually released. The receding safety buffer allows proposals to slowly become more risky as we gather observations of $\vec{V}$. In our experiments, we relate the number of edge cells in the safety buffer to the number of drifters already deployed, n. The number of edge cells zeroed in Φ is calculated by $((n*(\min(m,n)-b_n)/n_d)+b_n)$ for each drifter deployment, with the minimum edge buffer, b_n, chosen to be 10 cells. Next, each point in Φ which has already been observed by a deployed drifter is set to 0. Then $\frac{1}{n_f}$ is subtracted from Φ for each point in $\hat{D}$. Lastly, a dilation is performed over Φ which smears the boundaries of the drifter tracks, discouraging proposal points near deployed trajectories.

Rejection sampling is performed on all of the coordinates in Φ until we've acquired 1000 unique points in R. We further prune this set of points using a fast spatial filtering process known as non-maximum suppression (NMS) until we have p_n promising points ($p_n = 100$ in our experiments). NMS works by greedily selecting high-value proposals while deleting nearby proposals which cover the same area [38]. Our proposal approach was inspired by modern object recognition systems in image processing pipelines such as [39] in which an object detector proposes many windows around each object in an image and then the windows are thinned out based on their overlap by NMS to produce the most likely window directly over an object. The proposal points resulting from this process are pictured as yellow points in Figure 2b over Φ.

D. Deployment Point Selection

At this step in the deployment pipeline, we have filtered the set of potential deployment points down to a manageable number of points, p. To select the best p, we estimate trajectories for each p under $\hat{V}$ (an example of this step is shown in Figure 2c). Each proposal point's trajectory, $\hat{P}_n$, is scored by summing the unique points in R that are visited with respect to a *value field*, Γ. Γ is the same as Φ, except that the receding safety border is replaced with a narrow, fixed zero-value border, b_n to remove value from risky edge deployments. In our experiments, we found $b_n = 10$ to be reasonable, but this parameter can be adjusted. Scored proposal points are depicted in Figure 2d with yellow markers which reflect the relative score of a point. The proposal point with the highest value score is selected and the USV is instructed to drive to this deployment point to offload the next drifter. In our experiments, the ASV waits for 5 minutes before considering the next deployment.

V. Experimental Setup

While we have conducted several deployments in open water with this approach, the work in this paper places an emphasis on the quantitative impact of our trajectory modeling algorithm. Thus, in order to obtain large-scale statistically-valid quantitative results under ground truth, we report an analysis using archival geophysical flow fields with simulated sensor and vehicle placements.

We compare the performance of our approach over 40 Regional Ocean Modeling Systems (ROMS) [40] forecast flow fields for the Norweigian Sea. The data set consists of an array of 100×155 measurements of in-situ ocean current. In the original dataset, each data point was separated by $800m$, but we rescaled the spacing between sample points to correspond to a measurement interval of $5m$ so as to make the survey area small enough to be feasibly traversed by a typical ASV and so that our assumptions of a steady flow field were reasonable. This change made our testbed, R, equal to a size of $500m \times 775m$.

For each simulation, we initialize a simulated ASV with an average speed of $3m/s$ to an initial position of $(0, 0)$. The ASV begins each survey with n_d=10 drifters and must decide where to place each of them. When the ASV chooses a deployment point, our simulator generates 10 plausible paths based on the ground truth flow field that are 8 hours in length from the requested deployment point and randomly assigns one of these paths to the newly "deployed" drifter. The boat pauses for 30 seconds to release the drifter before considering

the deployment point for the next drifter. Each released drifter will sample the flow field at twice the Nyquist rate for the flow field until it exits R. In these experiments, we add a 1e-6 normal noise factor to each current observation. We assume that neither the flow field nor the drifter load have any effect on the speed of the ASV. An experiment terminates when all drifters have left R or after 8 hours.

We compared our approach to four nominal baselines. These baselines are referred to as: *highest variance*, *distributed long axis*, *distributed short axis*, and *random*. All deployment schemes deploy the first drifter into the center of the map to start the survey. None of the approaches allow placing drifters within b_n cells of the border of the survey where $b_n = 10$. In the variance baseline, at each deployment, the drifter is deployed to the coordinate in U containing the highest value and then the ASV pauses for 5 minutes while waiting for drifter observations. In the distributed and random baselines, there is no ASV wait time between deployments because drifter observations are not considered. For the distributed baselines, we deploy drifters evenly along the center of the axis specified in the deployment name. In random deployment, points are selected randomly without replacement from the set of points in R. Figure 4 demonstrates the each of the deployment strategies.

VI. Results and Discussion

Results from the experiments described in the previous section can be seen in Figure 3. Our approach covered the most unique cells in 92.5% (37 out of the 40) flow fields. Variance, distributed long, and distributed short each were the highest performing deployment schemes on one of the 40 flow fields. The flow fields in which our approach struggled contained eddies and regions with low current that were difficult to model correctly. Although the variance based deployment occasionally produced a better estimate of $\vec{V}$ in a shorter amount of time, it often squandered drifters by deploying them at points which guaranteed they had short trajectories.

Although we strove to reduce computational requirement to make our planning approach tractable, it still requires significant compute, particularly in the data assimilation and trajectory prediction phases. Each deployment calculation takes approximately 30 seconds (depending on the number of points in $\bar{D}$) on a modern desktop. In these experiments, we always pause for a constant time after a deployment to allow for data collection, however, in future experiments, we think this pause time should be a parameter that responds to the observations of the deployed drifters. Future work will also consider non-steady flow fields and drifter networks with non-uniform physical characteristics.

VII. Conclusion

In this paper, we presented an approach for effectively deploying low-cost sensors in an unknown flow field so as to optimize coverage where are objective is to simultaneously exploit the flow field and to model it. By combining real-time modeling with these passive sensors we demonstrate

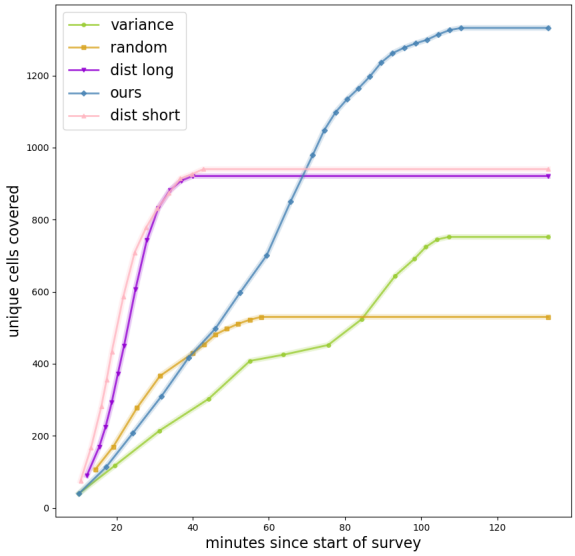

Fig. 5: Comparison of deployment schemes on the flow field depicted in Figure 4 over time. A higher number of unique cells covered is desirable.

that we can achieve reasonable performance when compared to baseline algorithms. Since currents are often modeled as ergodic processes, the effectiveness of this approach is substantial for applications which can accept temporal constraints on drifter motion.

We think this autonomous monitoring technique will be of value for scientists completing marine surveys because it is highly mobile, configurable, and can be deployed with minimal investment in infrastructure. In future work, we intend to investigate task sharing between the passive sensors and ASV and active drifter deployment schemes.

Acknowledgment

This work would not have been possible without tremendous support from our colleagues, especially Sandeep Manjanna. We thank Alberto Quattrini Li, Ioannis Rekleitis, and Ryan Smith for their correspondence and for graciously allowing us to use their equipment and facilities to conduct related field experiments. We also gratefully acknowledge the support of the National Science and Engineering Research Council of Canada and our industrial partners including Clearpath Robotics.

References

[1] H. U. Sverdrup, M. W. Johnson, and R. H. Fleming, *The oceans, their physics, chemistry, and general biology, by H. U. Sverdrup, Martin W. Johnson and Richard H. Fleming*. Prentice-Hall, inc New York, 1942.

[2] N. N. Soreide, C. E. Woody, and S. M. Holt, "Overview of ocean based buoys and drifters: present applications and future needs," in *MTS/IEEE Oceans 2001. An Ocean Odyssey. Conference Proceedings (IEEE Cat. No.01CH37295)*, vol. 4, 2001, pp. 2470–2472 vol.4.

[3] R. Lumpkin, M. Pazos, N. Oceanographic, and A. Administration, "Measuring surface currents with surface velocity program drifters: the instrument, its data, and some recent results. chapter two of lagrangian analysis," in *and Prediction of Coastal and Ocean Dynamics*. University Press, 2007.

[4] E. W. Blockley, M. J. Martin, and P. Hyder, "Validation of foam near-surface ocean current forecasts using lagrangian drifting buoys," *Ocean Science*, vol. 8, no. 4, pp. 551–565, 2012. [Online]. Available: https://www.ocean-sci.net/8/551/2012/

[5] N. Maximenko, J. Hafner, and P. Niiler, "Pathways of marine debris derived from trajectories of lagrangian drifters," *Marine Pollution Bulletin*, vol. 65, no. 1, pp. 51 – 62, 2012, at-sea Detection of Derelict Fishing Gear. [Online]. Available: http://www.sciencedirect.com/science/article/pii/S0025326X11002189

[6] I. I. Rypina, S. R. Jayne, S. Yoshida, A. M. Macdonald, and K. Buesseler, "Drifter-based estimate of the 5 year dispersal of fukushima-derived radionuclides," *Journal of Geophysical Research: Oceans*, vol. 119, no. 11, pp. 8177–8193, 2014. [Online]. Available: http://dx.doi.org/10.1002/2014JC010306

[7] R. Brainard, R. Moffitt, M. Timmers, G. Paulay, L. Plaisance, N. Knowlton, J. Caley, F. Fohrer, A. Charette, C. Meyer, *et al.*, "Autonomous reef monitoring structures (arms): A tool for monitoring indices of biodiversity in the pacific islands," in *11th Pacific Science Inter-Congress, Papeete, Tahiti*, 2009.

[8] S. B. Williams, O. Pizarro, J. M. Webser, R. J. Beaman, I. Mahon, M. Johnson-Roberson, and T. Bridge, "AUV-assisted Surveying of Drowned Reefs on the Shelf Edge of the Great Barrier Reef, Australia," *Journal of Field Robotics*, vol. 27, no. 5, pp. 675–697, 2010.

[9] O. Pizarro, S. B. Williams, M. Johnson-Roberson, D. Steinberg, and M. Bryson, "Reef mapping and monitoring assisted by machines," in *Ocean Sciences 2014 Meeting*, 2014.

[10] Y. Girdhar and G. Dudek, "Modeling curiosity in a mobile robot for long-term autonomous exploration and monitoring," *Autonomous Robots*, vol. 40, no. 7, pp. 1267–1278, 10 2016.

[11] S. Manjanna, J. Hansen, A. Q. Li, I. Rekleitis, and G. Dudek, "Collaborative sampling using heterogeneous marine robots driven by visual cues," in *2017 14th Conference on Computer and Robot Vision (CRV)*, June 2017.

[12] H. SALMAN, K. IDE, and C. K. R. T. JONES, "Using flow geometry for drifter deployment in lagrangian data assimilation," *Tellus A*, vol. 60, no. 2, pp. 321–335, 2008. [Online]. Available: http://dx.doi.org/10.1111/j.1600-0870.2007.00292.x

[13] G. A. Hollinger and G. S. Sukhatme, "Sampling-based motion planning for robotic information gathering," in *Robotics: Science and Systems*, Jun 2013. [Online]. Available: http://robotics.usc.edu/publications/841/

[14] X. Wu, M. Liu, and Y. Wu, "In-situ soil moisture sensing: Optimal sensor placement and field estimation," *ACM Trans. Sen. Netw.*, vol. 8, no. 4, pp. 33:1–33:30, Sept. 2012. [Online]. Available: http://doi.acm.org/10.1145/2240116.2240122

[15] M. Rahimi, M. Hansen, W. J. Kaiser, G. S. Sukhatme, and D. Estrin, "Adaptive sampling for environmental field estimation using robotic sensors," in *2005 IEEE/RSJ International Conference on Intelligent Robots and Systems*, Aug 2005, pp. 3692–3698.

[16] R. N. Smith, Y. Chao, P. P. Li, D. A. Caron, B. H. Jones, and G. S. Sukhatme, "Planning and implementing trajectories for autonomous underwater vehicles to track evolving ocean processes based on predictions from a regional ocean model," *The International Journal of Robotics Research*, p. 0278364910377243, 2010.

[17] D. Kularatne and A. Hsieh, "Tracking attracting lagrangian coherent structures in flows," in *Proceedings of Robotics: Science and Systems*, Rome, Italy, July 2015.

[18] D. Kularatne, S. Bhattacharya, and M. A. Hsieh, "Optimal path planning in time-varying flows using adaptive discretization," *IEEE Robotics and Automation Letters*, vol. 3, no. 1, pp. 458–465, Jan 2018.

[19] M. Meghjani, S. Manjanna, and G. Dudek, "Multi-target rendezvous search," in *IEEE/RSJ International Conference on Intelligent Robots and Systems (IROS), 2016*. IEEE, 2016, pp. 2596–2603.

[20] F. Shkurti, A. Xu, M. Meghjani, J. C. G. Higuera, Y. Girdhar, P. Giguere, B. B. Dey, J. Li, A. Kalmbach, C. Prahacs, K. Turgeon, I. Rekleitis, and G. Dudek, "Multi-domain monitoring of marine environments using a heterogeneous robot team," in *IEEE/RSJ International Conference on Intelligent Robots and Systems*, Portugal, Oct. 2012, pp. 1447–1753.

[21] J. Das, F. Py, T. Maughan, T. OReilly, M. Messi, J. Ryan, G. S. Sukhatme, and K. Rajan, "Coordinated sampling of dynamic oceanographic features with underwater vehicles and drifters," *The International Journal of Robotics Research*, vol. 31, no. 5, pp. 626–646, 2012. [Online]. Available: https://doi.org/10.1177/0278364912440736

[22] A. A. Pereira, J. Binney, G. A. Hollinger, and G. S. Sukhatme, "Risk-aware path planning for autonomous underwater vehicles using predictive ocean models," *Journal of Field Robotics*, vol. 30, no. 5, pp. 741–762, 2013. [Online]. Available: http://dx.doi.org/10.1002/rob.21472

[23] N. E. Leonard, D. A. Paley, F. Lekien, R. Sepulchre, D. M. Fratantoni, and R. E. Davis, "Collective motion, sensor networks, and ocean sampling," *Proceedings of the IEEE*, vol. 95, no. 1, pp. 48–74, Jan 2007.

[24] T. Inanc, S. C. Shadden, and J. E. Marsden, "Optimal trajectory generation in ocean flows," in *Proceedings of the 2005, American Control Conference, 2005.*, June 2005, pp. 674–679.

[25] M. Ouimet and J. Corts, "Coordinated rendezvous of underwater drifters in ocean internal waves," in *53rd IEEE Conference on Decision and Control*, Dec 2014, pp. 6099–6104.

[26] A. Molchanov, A. Breitenmoser, and G. S. Sukhatme, "Active drifters: Towards a practical multi-robot system for ocean monitoring," in *2015 IEEE International Conference on Robotics and Automation (ICRA)*, May 2015, pp. 545–552.

[27] A. Molcard, A. Poje, and T. zgkmen, "Directed drifter launch strategies for lagrangian data assimilation using hyperbolic trajectories," *Ocean Modelling*, vol. 12, no. 3-4, pp. 268–289, 2006.

[28] A. A. Allen and C. B. Billing, "Spatial objective analysis of small numbers of lagrangian drifters," in *OCEANS '88. A Partnership of Marine Interests. Proceedings*, Oct 1988, pp. 860–864 vol.3.

[29] H. Salman, L. Kuznetsov, C. K. R. T. Jones, and K. Ide, "A method for assimilating lagrangian data into a shallow-water-equation ocean model," *Monthly Weather Review*, vol. 134, no. 4, pp. 1081–1101, 2006. [Online]. Available: https://doi.org/10.1175/MWR3104.1

[30] M. Kamachi and J. O'Brien, "Continuous data assimilation of drifting buoy trajectory into an equatorial pacific ocean model," *Journal of Marine Systems*, vol. 6, no. 1, pp. 159 – 178, 1995, data Assimilation in Manine Science. [Online]. Available: http://www.sciencedirect.com/science/article/pii/0924796394000224

[31] A. Tinka, I. Strub, Q. Wu, and A. M. Bayen, "Quadratic programming based data assimilation with passive drifting sensors for shallow water flows," in *Proceedings of the 48h IEEE Conference on Decision and Control (CDC) held jointly with 2009 28th Chinese Control Conference*, Dec 2009, pp. 7614–7620.

[32] W. Sun, N. Sood, D. Dey, G. Ranade, S. Prakash, and A. Kapoor, "No-regret replanning under uncertainty," in *2017 IEEE International Conference on Robotics and Automation (ICRA)*, May 2017, pp. 6420–6427.

[33] A. Singh, F. Ramos, H. D. Whyte, and W. J. Kaiser, "Modeling and decision making in spatio-temporal processes for environmental surveillance," in *2010 IEEE International Conference on Robotics and Automation*, May 2010, pp. 5490–5497.

[34] Y. Zhao, F. Yin, F. Gunnarsson, F. Hultkratz, and J. Fagerlind, "Gaussian processes for flow modeling and prediction of positioned trajectories evaluated with sports data," in *2016 19th International Conference on Information Fusion (FUSION)*, July 2016, pp. 1461–1468.

[35] K. Kim, D. Lee, and I. Essa, "Gaussian process regression flow for analysis of motion trajectories," in *2011 International Conference on Computer Vision*, Nov 2011, pp. 1164–1171.

[36] S. Reece, R. Mann, I. Rezek, and S. Roberts, "Gaussian Process Segmentation of Co-Moving Animals," in *American Institute of Physics Conference Series*, ser. American Institute of Physics Conference Series, A. Mohammad-Djafari, J.-F. Bercher, and P. Bessiére, Eds., vol. 1305, Mar. 2011, pp. 430–437.

[37] K.-F. Dagestad, J. Röhrs, Ø. Breivik, and B. Ådlandsvik, "Opendrift v1.0: a generic framework for trajectory modeling," *Geoscientific Model Development Discussions*, vol. 2017, pp. 1–28, 2017. [Online]. Available: https://www.geosci-model-dev-discuss.net/gmd-2017-205/

[38] A. Rosenfeld and M. Thurston, "Edge and curve detection for visual scene analysis," *IEEE Transactions on Computers*, vol. C-20, no. 5, pp. 562–569, May 1971.

[39] S. Ren, K. He, R. Girshick, and J. Sun, "Faster r-cnn: Towards real-time object detection with region proposal networks," in *Advances in Neural Information Processing Systems 28*, C. Cortes, N. D. Lawrence, D. D. Lee, M. Sugiyama, and R. Garnett, Eds. Curran Associates, Inc., 2015, pp. 91–99. [Online]. Available: http://papers.nips.cc/paper/5638-faster-r-cnn-towards-real-time-object-detection-with-region-proposal-networks.pdf

[40] A. F. Shchepetkin and J. C. McWilliams, "The regional oceanic modeling system (ROMS): a split-explicit, free-surface, topography-following-coordinate oceanic model," *Ocean Modelling*, vol. 9, pp. 347–404, 2005.